Correlation of Na^+/I^- Symporter Expression and Activity: Implications of Na^+/I^- Symporter as an Imaging Reporter Gene

Douangsone D. Vadysirisack, BS[1,2]; Daniel H. Shen, MD, PhD[3]; and Sissy M. Jhiang, PhD[1,2,4]

[1]Integrated Biomedical Science Graduate Program, Ohio State University, Columbus, Ohio; [2]Department of Physiology and Cell Biology, Ohio State University, Columbus, Ohio; [3]Department of Nuclear Medicine, Tri-Service General Hospital, National Defense Medical Center, Taipei, Taiwan; and [4]Department of Internal Medicine, Ohio State University, Columbus, Ohio

The Na^+/I^- symporter (NIS) has been proposed as an imaging reporter gene to ascertain the expression of therapeutic genes in targeted tissues. In this study, we investigated whether posttranslational processing and cell-surface trafficking of NIS affect NIS-mediated radioiodide uptake in cells expressing exogenous NIS. **Methods:** We established FTC133, HeLa, and PC12 cell lines with doxycycline-inducible NIS expression to investigate the correlation among total NIS protein levels, cell-surface NIS protein levels, and NIS-mediated radioiodide uptake in cells induced with various levels of NIS. **Results:** We found that most exogenous NIS proteins were efficiently trafficked to the cell surface; thus, a possible deficiency in NIS cell-surface trafficking is not a concern for clinical applications of NIS gene transfer. The extent of radioiodide uptake correlated with cell-surface NIS protein level within a certain range, suggesting that the imaging signals can quantify levels of NIS expression only within a certain range in vivo. Finally, a moderate increase in NIS protein level significantly increased radioiodide uptake, indicating that a low level of NIS expression is sufficient to facilitate radionuclide imaging in vivo. **Conclusion:** Our study suggests that NIS will be useful as an imaging reporter gene to ascertain that the therapeutic gene is localized to the correct tissue and to monitor the expression levels and duration of the therapeutic gene.

Key Words: sodium iodide symporter; NIS; imaging reporter gene; cell-surface trafficking

J Nucl Med 2006; 47:182–190

Gene therapy may provide additional therapeutic options for conditions such as genetic disorders, metabolic diseases, and cancer (*1,2*). Despite progress in current clinical gene therapy trials, problems still exist with inefficient vector delivery and tissue targeting. The development of simple and specific ways to noninvasively and repetitively image exogenous gene delivery and expression will greatly advance the field of gene therapy. One such way to monitor gene delivery and expression involves the inclusion of an imaging reporter gene (Imagene) in the gene therapy vector (*3–5*). Imaging reporter genes code for a protein that mediates a specific interaction with a detectable substrate, allowing a clinician or investigator to determine whether the therapeutic gene has successfully been delivered, whether the therapeutic gene is localized to the correct tissue, whether the expression level of the therapeutic gene is sufficient for therapy, and the duration of gene expression (*3–5*). The use of imaging reporter genes will be instrumental in the development of new strategies and reagents for targeted, effective gene therapy.

One of the most promising types of imaging reporter gene is the Na^+/I^- symporter (NIS). NIS is an intrinsic membrane glycoprotein with 13 putative transmembrane domains. Electrophysiologic studies have shown that NIS functions by cotransporting 1 I^- ion with 2 Na^+ ions into cells (*6*). In addition, other molecules, such as TcO_4^-, are readily transported by NIS. As a result, cells that express NIS will concentrate I^- and TcO_4^-, and this uptake and intracellular accumulation can be detected using radiotracer ^{131}I, ^{123}I, ^{125}I, or $^{99m}TcO_4$ (*7*). Indeed, several published reports have demonstrated that NIS expression can effectively be imaged in vivo (*7–15*).

We and others have demonstrated that NIS gene transfer can facilitate radioiodide uptake in a variety of cells; however, the extent of radioiodide uptake varies considerably among different cell types (*16–22*). The mechanisms underlying this difference have not been investigated. The aim of this study was to determine whether posttranslational processing and cell-surface trafficking of NIS affect NIS-mediated radioiodide uptake in cells expressing exogenous NIS. Furthermore, the correlations among total NIS protein levels, cell-surface NIS protein levels, and NIS-mediated radioiodide uptake were investigated and compared among 3 different types of cells expressing various NIS levels. The information acquired should facilitate future applications of NIS as an imaging reporter gene in clinical trials.

Received May 27, 2005; revision accepted Aug. 8, 2005.

For correspondence or reprints contact: Sissy M. Jhiang, PhD, 304 Hamilton Hall, 1645 Neil Ave., Ohio State University, Columbus, OH 43210.
E-mail: jhiang.1@osu.edu

MATERIALS AND METHODS

Cell Culture

FTC133 human thyroid cancer cells were maintained in 1:1 Dulbecco's modified Eagle's medium (DMEM):modified Ham's F12 medium (Invitrogen) supplemented with fetal bovine serum (10%; Invitrogen), glutamine (2 mmol/L; Invitrogen), penicillin/streptomycin (1%; Invitrogen), and a mixture of bovine thyroid-stimulating hormone (1 mU/mL; Sigma) and bovine insulin (10 μg/mL; Sigma). HeLa human cervical cancer cells were maintained in DMEM supplemented with fetal bovine serum (10%) and penicillin/streptomycin (1%). PC12 rat pheochromocytoma cells were maintained in DMEM supplemented with horse serum (10%; Invitrogen), fetal bovine serum (5%), glutamine (2 mmol/L), and penicillin/streptomycin (1%). Phoenix retroviral producer cells were maintained in DMEM supplemented with fetal bovine serum (10%) and penicillin/streptomycin (1%). Cells stably expressing CMV-TetOn and TREhNIS were maintained in medium supplemented with G418 (200 μg/mL; Gibco) and hygromycin (100 μg/mL; Clontech).

Generation of TetOn/NIS Cell Lines

Full-length human NIS in pCDNA3 vector was released with BamHI and EcoRV and then subcloned into BamHI- and HpaI-digested pRev-TRE (Clontech). Phoenix cells were transfected with pRev-TREhNIS, and retroviruses were harvested. HeLa TetOn and PC12 TetOn cells (Clontech) were transduced with pRev-TREhNIS retroviral supernatant, and stable clones were selected in medium containing hygromycin (200 μg/mL). For generation of FTC133 TetOn cells, parental cells were stably transfected with CMV-TetOn (Clontech) and selected in medium containing G418 (400 μg/mL). Clones were screened for functional expression of TetOn by transient transfection of pRev-TREhNIS, followed by radioiodide uptake assay. Selected FTC133 TetOn clones were then transduced with pRev-TREhNIS retroviral supernatant to isolate FTC133 TetOn/NIS clones. All TetOn/NIS clones were selected on the basis of low leakiness and high doxycycline-inducible NIS expression by radioiodide uptake assay.

Radioiodide Uptake Assay

Uptake of ^{125}I was measured as described previously (*23*). Briefly, TetOn/NIS cells were seeded in 24-well plates 24 h before the addition of doxycycline. FTC133 TetOn/NIS cells and HeLa TetOn/NIS cells were induced with 0, 0.1, 0.5, or 2 μg of doxycycline per milliliter, and PC12 TetOn/NIS cells were induced with 0, 0.05, 0.2, or 1 μg of doxycycline per milliliter. Forty-eight hours later, cells were incubated with 74 kBq of $Na^{125}I$ in 5 μmol of nonradioactive NaI per liter for 30 min at 37°C with 5% CO_2. Cells were then washed twice with cold Hanks' balanced salt solution (HBSS) and lysed with cold 95% ethanol for 20 min at room temperature. The cell lysate was collected, and radioactivity was counted by a γ-counter (Packard Instruments). Experiments were performed in triplicate.

Iodide Efflux Assay

Efflux of ^{125}I was measured as described previously (*23*). FTC133 TetOn/NIS cells and HeLa TetOn/NIS cells were induced with 2 μg of doxycycline per milliliter, whereas PC12 TetOn/NIS cells were induced with 1 μg of doxycycline per milliliter. Forty-eight hours later, cells were incubated in medium containing $Na^{125}I$ as described above. Cells were washed twice and incubated in 1 mL of HBSS. After 2 min, the medium was collected and replaced with HBSS. This was repeated every 2 min for a total of 10 min. Cells were then lysed with cold 95% ethanol for 20 min at room temperature. The total uptake of each well was calculated as the sum of the efflux washes and the lysate. Experiments were performed in triplicate.

Cell-Surface Biotinylation

TetOn/NIS cells were seeded in 100-mm plates and induced with doxycycline for 48 h. Cell-surface biotinylation was performed by washing the cells with cold phosphate-buffered saline (PBS) containing $MgCl_2$ (1 mmol/L) and $CaCl_2$ (0.1 mmol/L) (PBS Ca/Mg). The cells were then incubated with sulfo-NHS-LC-biotin (1 mg/mL; Pierce) in PBS Ca/Mg for 1 h with gentle shaking at 4°C. The reaction was quenched with PBS Ca/Mg containing glycine (20 mmol/L) for 20 min at 4°C. Cells were then lysed in lysis buffer (Tris, 50 mmol/L, pH 7.5; NaCl, 150 mmol/L; Triton X-100, 1%; phenylmethylsulfonyl fluoride, 1 mmol/L; aprotinin, 10 μg/mL; leupeptin, 10 μg/mL) for 30 min at 4°C. An 18.5-gauge needle was used to homogenize the cells. Next, lysates were centrifuged at 14,000*g* for 20 min at 4°C and supernatants (whole-cell lysates) were collected. Protein concentrations were determined by Bradford assay (Bio-Rad). For separation of biotinylated proteins from nonbiotinylated proteins, 800 μg of whole-cell lysates were incubated with 100 μL of avidin-coated agarose beads (Pierce) overnight with gentle shaking at 4°C. The beads were then washed with lysis buffer, and biotin-labeled proteins were eluted with 75 μL of 2× Laemmli sample buffer for 5 min at 95°C. Aliquots (20 μg) of whole-cell lysates were used to assess total NIS protein levels. Proteins were subjected to Western blot analysis as described below. To ensure that biotin did not permeate the cells and label intracellular proteins, we probed the membrane with a rabbit polyclonal α-actin antibody (Santa Cruz) at a 1:500 dilution. Actin was detected in the total NIS protein fractions but not in the cell-surface NIS fractions (data not shown).

Western Blot Analysis

Proteins were subjected to 10% sodium dodecylsulfate–polyacrylamide gel electrophoresis and transferred to a nitrocellulose membrane (Schleicher and Schuell). The membrane was blocked in Tris-buffered saline polysorbate (Tris-HCl, 10 mmol/L, pH 8.0; NaCl, 150 mmol/L; polysorbate 20, 0.05%) containing 5% nonfat dry milk either for 1 h at room temperature or overnight at 4°C. Next, the membrane was incubated with 331 polyclonal rabbit α-human NIS antibody diluted 1:1,500 for 1 h at room temperature, followed by incubation with horseradish peroxidase–conjugated α-rabbit IgG (Amersham Pharmacia), diluted 1:4,000 for 1 h at room temperature. The signal was detected by an enhanced chemiluminescence detection reagent (Amersham). The signal intensities were measured densitometrically using NIH *Image* software (National Institute of Mental Health). To determine equal protein loading of total NIS proteins and cell-surface NIS proteins, we probed the membrane with an antibody against vascular adenosine triphosphatase (V-ATPase) E subunit (kindly provided by Dr. Beth Lee, Ohio State University) diluted 1:1,000, followed by incubation with horseradish peroxidase–conjugated α-rabbit IgG.

Adenovirus-Mediated NIS Transduction

Generation of recombinant adenovirus carrying human NIS (rAdCMVFLhNIS) has been described previously (*18*). Twenty-four hours before infection, parental FTC133 cells and parental HeLa

cells were seeded in 24-well plates for radioiodide uptake assay or in 100-mm plates for cell-surface biotinylation. For adenovirus-mediated NIS transduction, cells were washed with PBS, incubated with 2% fetal bovine serum, and infected with a multiplicity of infection of 0, 1, 3, or 10 for 2 h. Afterward, cells were washed with PBS and cultured in regular medium. Forty-eight hours after infection, radioiodide uptake assay and Western blot analysis were performed as described above.

Statistical Analysis

The correlation coefficient (r) for the statistical comparison of total NIS protein levels with cell-surface NIS levels was determined. A P value of less than 0.05 was considered to be statistically significant.

RESULTS

Doxycycline-Inducible NIS Expression Is Established in 3 Cell Lines of Different Tissue Types

Doxycycline-inducible NIS expression was established in 3 cell lines of different tissue types, FTC133 human thyroid cancer cells, HeLa human cervical cancer cells, and PC12 rat pheochromocytoma cells. These parental cell lines do not express endogenous NIS and thus do not actively transport radioiodide. All 3 TetOn/NIS cells, stably ex-

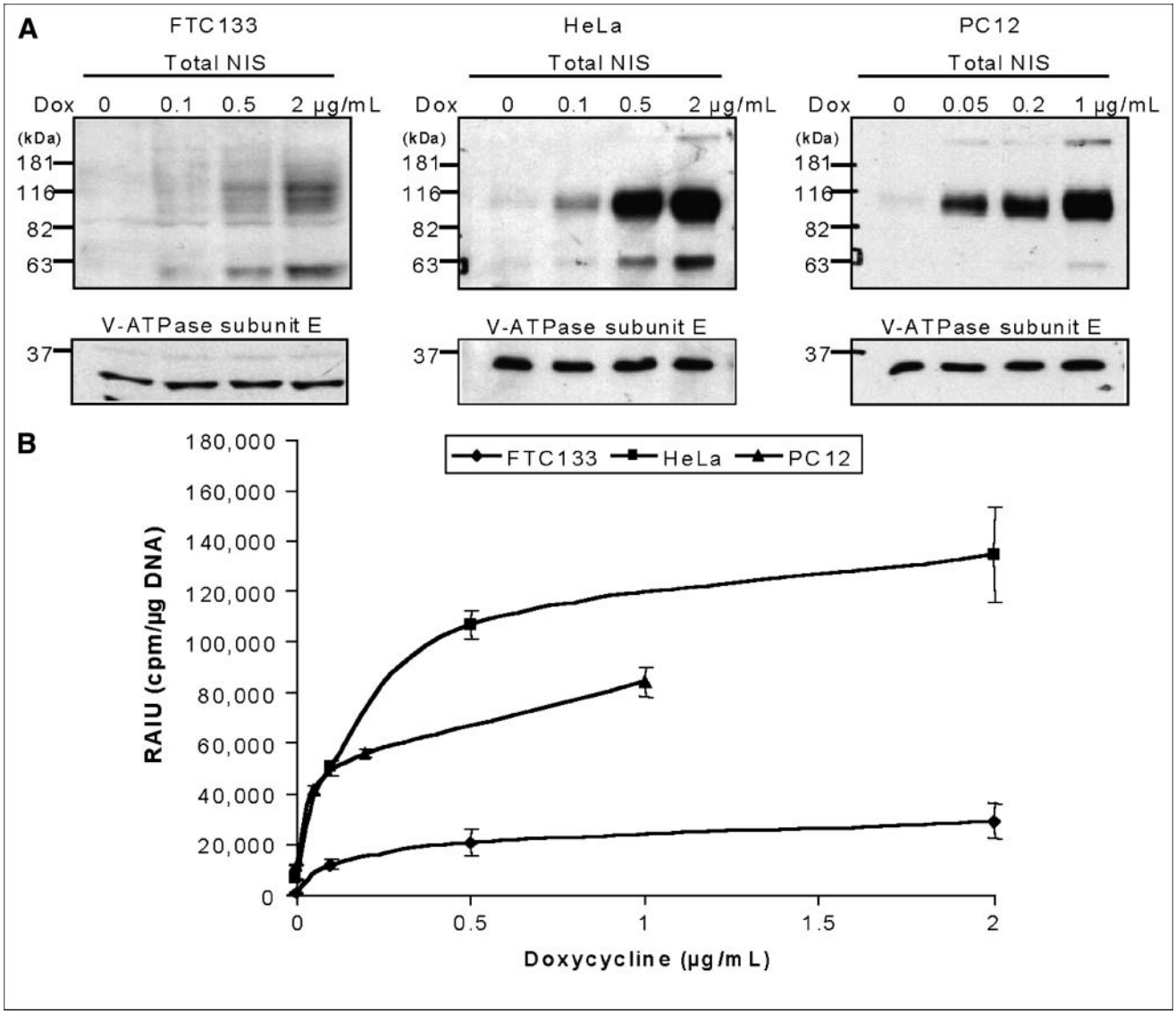

FIGURE 1. Doxycycline-inducible NIS expression and radioiodide uptake. (A) Western blot analysis showed that maximal inducible NIS protein level was higher in HeLa TetOn/NIS cells and PC12 TetOn/NIS than in FTC133 TetOn/NIS cells. All TetOn/NIS cells were induced for 48 h with various doxycycline concentrations. Equal loading of proteins was normalized with V-ATPase. Exposure time for detecting NIS protein in FTC133 TetOn/NIS was 30 min, whereas exposure time for HeLa TetOn/NIS and PC12 TetOn/NIS cells was 5 min. Results are representative of 3 independent experiments. (B) Extent of radioiodide uptake generally correlates with level of inducible NIS proteins. Each data point was performed in triplicate, and mean ± SD are shown. Results are representative of 3 independent experiments. RAIU = radioiodide uptake.

pressing the reverse tetracycline transactivator (TetOn) and NIS linked to a tetracycline-responsive element, had doxycycline-inducible NIS expression (Fig. 1A) and radioiodide uptake (Fig. 1B). Low levels of NIS protein were detectable in the absence of doxycycline, indicating some leakiness of NIS expression in all 3 TetOn/NIS cells (Fig. 1A). Western blot analysis for total NIS protein levels showed 2 major immunoreactive bands. The 90-kDa band represents the mature glycosylated NIS protein, whereas the 65-kDa band corresponds to partially glycosylated NIS protein. Interestingly, a minor third band of ~181 kDa was detected in both HeLa TetOn/NIS and PC12 TetOn/NIS cells but not in FTC133 TetOn/NIS cells. On the basis of the molecular weight, the ~181-kDa immunoreactive band most likely represents dimeric forms of NIS (*24–26*).

As shown in Figure 1B, both FTC133 TetOn/NIS cells and HeLa TetOn/NIS cells reached maximal radioiodide uptake with 2 μg of doxycycline per milliliter. In comparison, PC12 TetOn/NIS cells achieved maximum iodide uptake with 1 μg of doxycycline per milliliter. Administration of 5 μg of doxycycline per milliliter did not further increase radioiodide uptake in the 3 TetOn/NIS cells (data not shown). The degree of maximal induced radioiodide accumulation was highest in HeLa TetOn/NIS cells and lowest in FTC133 TetOn/NIS cells. Consistent with this finding, the maximal induced NIS protein level was highest in HeLa TetOn/NIS cells and lowest in FTC133 TetOn/NIS cells (Fig. 1A). Furthermore, consistent with the leakiness of NIS expression, all 3 TetOn/NIS cells had low levels of perchlorate-sensitive NIS-mediated radioiodide uptake in the absence of doxycycline. Nevertheless, NIS protein levels and radioiodide uptake could be modulated by various concentrations of doxycycline in all 3 TetOn/NIS cell lines. Furthermore, it appears that the radioiodide uptake is proportional to the corresponding total NIS protein levels among the 3 TetOn/NIS cells.

Rate of Iodide Efflux Is Not Different Among the 3 TetOn/NIS Cells

Both active iodide uptake and iodide efflux contribute to steady-state radioiodide accumulation. We therefore examined the rate of iodide efflux in the 3 TetOn/NIS cells treated with 2 μg of doxycycline per milliliter. As shown in Figure 2, accumulated radioiodide was rapidly lost in induced HeLa TetOn/NIS, PC12 TetOn/NIS, and FTC133 TetOn/NIS cells, most likely because of the lack of iodide organification. The rate of iodide efflux was similar among the 3 TetOn/NIS cells, because all 3 cell lines lost 50% of accumulated iodide by 4 min. Thus, the difference in maximal radioiodide accumulation among the 3 TetOn/NIS cells was not caused by differences in the rate of iodide efflux.

NIS Proteins Efficiently Traffic to Cell Surface in TetOn/NIS Cells

It is the NIS protein localized at the cell surface, but not the total NIS protein levels, that determines the degree of NIS-mediated radioiodide uptake. To investigate whether there is

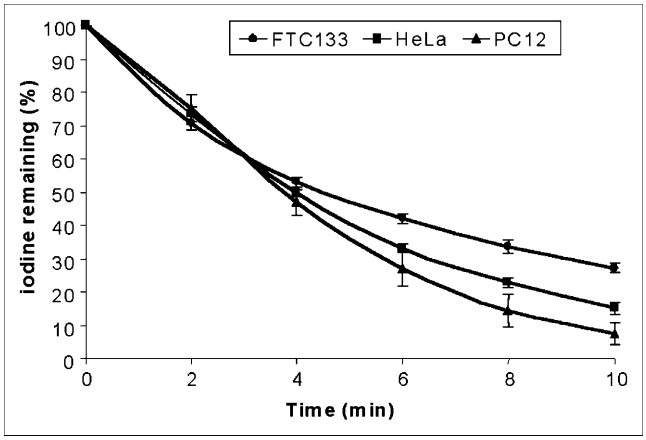

FIGURE 2. TetOn/NIS cells have similar rates of iodide efflux. TetOn/NIS cells were induced for 48 h with either 2 μg of doxycycline per milliliter for FTC133 TetOn/NIS and HeLa TetOn/NIS cells or 1 μg of doxycycline per milliliter for PC12 TetOn/NIS cells. Each data point was performed in triplicate, and mean ± SD are shown. Results are representative of 3 independent experiments.

a difference in NIS cell-surface trafficking efficiency, we correlated cell-surface NIS protein levels with total NIS protein levels in HeLa TetOn/NIS cells and PC12 TetOn/NIS cells induced with various concentrations of doxycycline. Cell-surface biotinylation, followed by isolation of biotinylated fractions with avidin-coated beads, was used to assess cell-surface NIS levels. Aliquots of whole-cell lysates from biotinylated cells were used to determine the corresponding total NIS protein levels. As expected, total NIS protein levels were modulated by various doxycycline concentrations, and the 90-kDa NIS was most abundant in both HeLa TetOn/NIS (Fig. 3A) and PC12 TetOn/NIS cells (Fig. 3C). Interestingly, although the 90-kDa NIS remained the most abundant form of NIS at the cell surface in HeLa TetOn/NIS cells, the ~181-kDa NIS was more abundant than the 90-kDa NIS at the cell surface in PC12 TetOn/NIS cells. Nevertheless, the ratio of 90-kDa NIS versus ~181-kDa NIS decreased in the cell-surface fractions in both TetOn/NIS cells. Thus, the putative dimeric NIS protein (181-kDa NIS) appears to be more efficiently targeted to the cell surface than is the monomeric glycosylated NIS protein (90-kDa NIS). The 65-kDa NIS was less abundant at the cell surface in both HeLa TetOn/NIS cells (Fig. 3A) and PC12 TetOn/NIS cells (Fig. 3C), suggesting that most underglycosylated NIS remains intracellular. Regardless of the different forms of NIS, the amount of cell-surface NIS levels appears to be proportional to the amounts of total NIS protein levels in both HeLa TetOn/NIS cells (Fig. 3B) and PC12 TetOn/NIS cells (Fig. 3D). This finding indicates that induced NIS proteins are efficiently targeted to the cell surface. This is consistent with the finding that radioiodide uptake closely correlates with total NIS protein levels in TetOn/NIS cells. Because of the low levels of induced NIS protein, we were not able to evaluate the correlation between cell-surface NIS levels and total NIS protein levels in FTC133 TetOn/NIS cells.

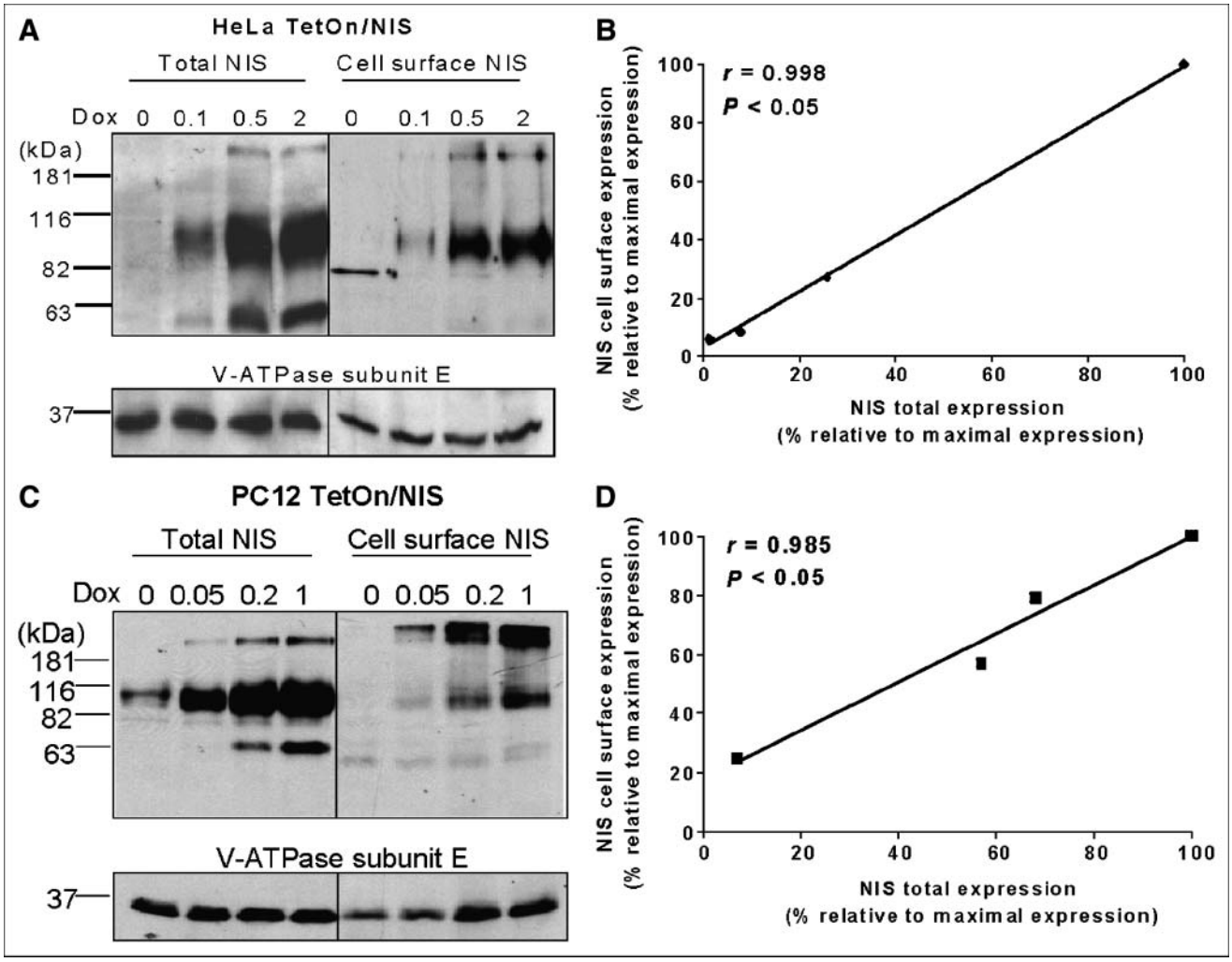

FIGURE 3. NIS protein efficiently traffics to cell surface in TetOn/NIS cells. (A and C) Total NIS protein levels correlate with cell-surface NIS levels in both HeLa TetOn/NIS cells (A) and PC12 TetOn/NIS cells (C). Cell-surface biotinylation followed by Western blot analysis using NIS antibodies was performed to detect cell-surface NIS levels, and aliquots of whole-cell lysates were used for Western blot analysis to determine total NIS protein levels. Ratio of 90-kDa NIS vs. ~181-kDa NIS decreases on surface of TetOn/NIS cells. TetOn/NIS cells were induced for 48 h with various doxycycline concentrations as indicated. Equal loading of proteins was normalized with V-ATPase. Exposure time was 5 min. Results are representative of 3 independent experiments. (B and D) Regression analysis indicates linear relationship between total NIS protein levels and cell-surface NIS levels in both HeLa TetOn/NIS cells (B) and PC12 TetOn/NIS cells (D). Densitometric analysis was performed to determine normalized total NIS protein levels and cell-surface NIS levels. To consolidate values from 3 independent experiments, maximally induced total NIS protein levels and maximally induced cell-surface NIS levels were designated as 100%, and other values were assigned relative to maximal levels. Correlation coefficient was determined. $P < 0.05$ indicates statistical significance. Dox = doxycycline.

A Moderate Increase in NIS Protein Results in a Marked Increase in Radioiodide Uptake

For the application of NIS as an imaging reporter gene or therapeutic gene, it is important to investigate the correlation between NIS protein levels and radioiodide uptake, because the degree of radioiodide uptake accounts for the imaging signals and therapeutic efficacy. Because cell-surface NIS levels appear to be proportional to total NIS protein levels, we next correlated cell-surface NIS protein levels with radioiodide uptake in both HeLa TetOn/NIS cells and PC12 TetOn/NIS cells. As shown in Figure 4, a moderate increase in NIS protein levels markedly increased radioiodide uptake. However, in both HeLa TetOn/NIS and PC12 TetOn/NIS cells, radioiodide uptake could not be further increased by further increases in NIS cell-surface levels beyond a certain range, indicating factors limiting NIS-mediated radioiodide uptake. These factors may include the availability of substrates I^- or Na^+. Increasing I^- concentrations from 5 to 15 μmol/L in the culture medium of HeLa TetOn/NIS cells further increased the extent of radioiodide uptake about 2-fold (data not shown). Interestingly, we found that the association between NIS protein levels and radioiodide uptake appeared to be different between HeLa TetOn/NIS and PC12 TetOn/NIS cells, in that the same amount of cell-surface NIS levels was associated with higher radioiodide uptake in HeLa TetOn/NIS than in PC12 TetOn/NIS cells.

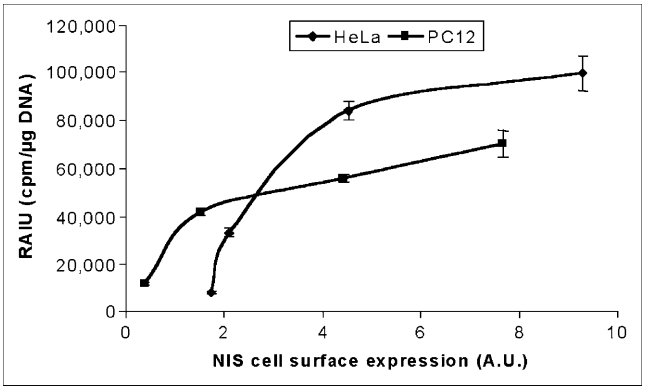

FIGURE 4. Extent of radioiodide uptake is not further increased by cell-surface NIS levels beyond a certain range in either HeLa TetOn/NIS or PC12 TetOn/NIS cells. Arbitrary values of cell-surface NIS levels were normalized with cell-surface V-ATPase levels and then correlated with corresponding radioiodide uptake. Results are representative of 3 independent experiments. A.U. = arbitrary units; RAIU = radioiodide uptake.

NIS Expression Level Is Not the Sole Factor Dictating Degree of Radioiodide Uptake

Several studies have demonstrated that the maximal radioiodide uptake induced by NIS gene transfer differs among different cells (*19–22*). However, the reasons underlying this difference have not been investigated, because NIS expression levels were not normalized among these cells. Using the TetOn/NIS cells, we found that the maximal radioiodide uptake differed among the different TetOn/NIS cells (Fig. 1B). To ensure that the finding was not due to clonal selection of the TetOn/NIS cells, we induced exogenous NIS expression at various levels in parental FTC133 or HeLa cells by infection with different amounts of recombinant adenovirus carrying NIS. Various NIS protein levels were conferred by infecting cells with differing multiplicities of infection of recombinant adenovirus–carrying NIS in both HeLa cells (Fig. 5A) and FTC133 cells (Fig. 5C). Consistent with the finding in the TetOn/NIS cells, the induced NIS proteins were efficiently targeted to the cell surface (Figs. 5B and 5D); a moderate increase in NIS cell-surface levels resulted in a marked increase in radioiodide uptake, yet further increases in NIS cell-surface level did not further increase radioiodide uptake (Fig. 6). Taken together, our study indicates that the level of NIS expression is not the sole factor dictating the degree of radioiodide uptake.

Unlike the finding in the TetOn/NIS cells, the maximal radioiodide uptake was higher in infected FTC133 cells than in infected HeLa cells (Fig. 6). In fact, at any equivalent NIS cell-surface levels, radioiodide uptake was always higher in infected FTC133 cells than in infected HeLa cells (Fig. 6). This finding indicates that the maximal radioiodide uptake in FTC133 TetOn/NIS cells does not reflect the maximal capacity of NIS-mediated radioiodide uptake in FTC133 cells. Instead, the low level of maximal radioiodide uptake in FTC133 TetOn/NIS cells was limited by the low level of inducible NIS protein in the selected clones.

DISCUSSION

NIS gene transfer by viral or nonviral approaches confers radioiodide uptake in a variety of murine and human cell lines; however, the extent of radioiodide uptake varies considerably among different cell types (*16–22*). The mechanisms underlying this difference have not been investigated. To examine the correlation between NIS protein levels and radioiodide uptake, we established TetOn/NIS cells of 3 different tissue types. The maximal radioiodide uptake correlated with the maximal induction of total NIS protein levels among the 3 TetOn/NIS cells. No differences in the rate of iodide efflux or NIS cell-surface targeting efficiency were observed among the 3 TetOn/NIS cells. What is most interesting is that for any given cell type, a moderate increase in NIS protein levels significantly increased radioiodide uptake, yet further increases in cell-surface NIS protein levels beyond a certain range could not further increase radioiodide uptake.

Several studies have shown that NIS cell-surface trafficking is quite susceptible to disruption. Clinically, some thyroid tumors have increased NIS expression yet fail to traffic or retain NIS at the cell surface; thus, these tumors cannot benefit from NIS-mediated radionuclide imaging or therapy (*27,28*). Furthermore, patients with defects in iodide transport often carry a mutation in NIS such that the NIS mutant fails to target to the cell surface (*29–32*). Experimentally, we found that NIS cell-surface trafficking is extremely susceptible to amino acid substitutions (*33*) and that the 5′ untranslated region of human NIS plays an important role in NIS cell-surface trafficking (Xiaoqin Lin et al., unpublished data, December 2003). Thus, it is generally believed that NIS cell-surface trafficking is a limiting factor for NIS-mediated radioiodide uptake in cells expressing exogenous NIS. In this study, we showed that NIS proteins were efficiently trafficked to the cell surface in both TetOn/NIS cells and cells infected with recombinant adenovirus–carrying NIS. Together with other reports showing significant increases in radioiodide uptake after NIS gene transfer in many cell types, a possible deficiency in NIS cell-surface trafficking is not a concern for clinical applications of NIS gene transfer.

It is of clinical importance that a moderate increase in NIS protein levels markedly increased radioiodide uptake but that radioiodide uptake could not be further increased by further increasing cell-surface NIS protein levels beyond a certain range. For NIS to serve as an imaging reporter gene, it is important to investigate whether a linear relationship exists between NIS gene expression and imaging signals. The intensity of the imaging signals is determined by the extent of radioiodide uptake but not by NIS protein levels. Our study indicates that NIS protein levels have a linear relationship with the extent of radioiodide uptake

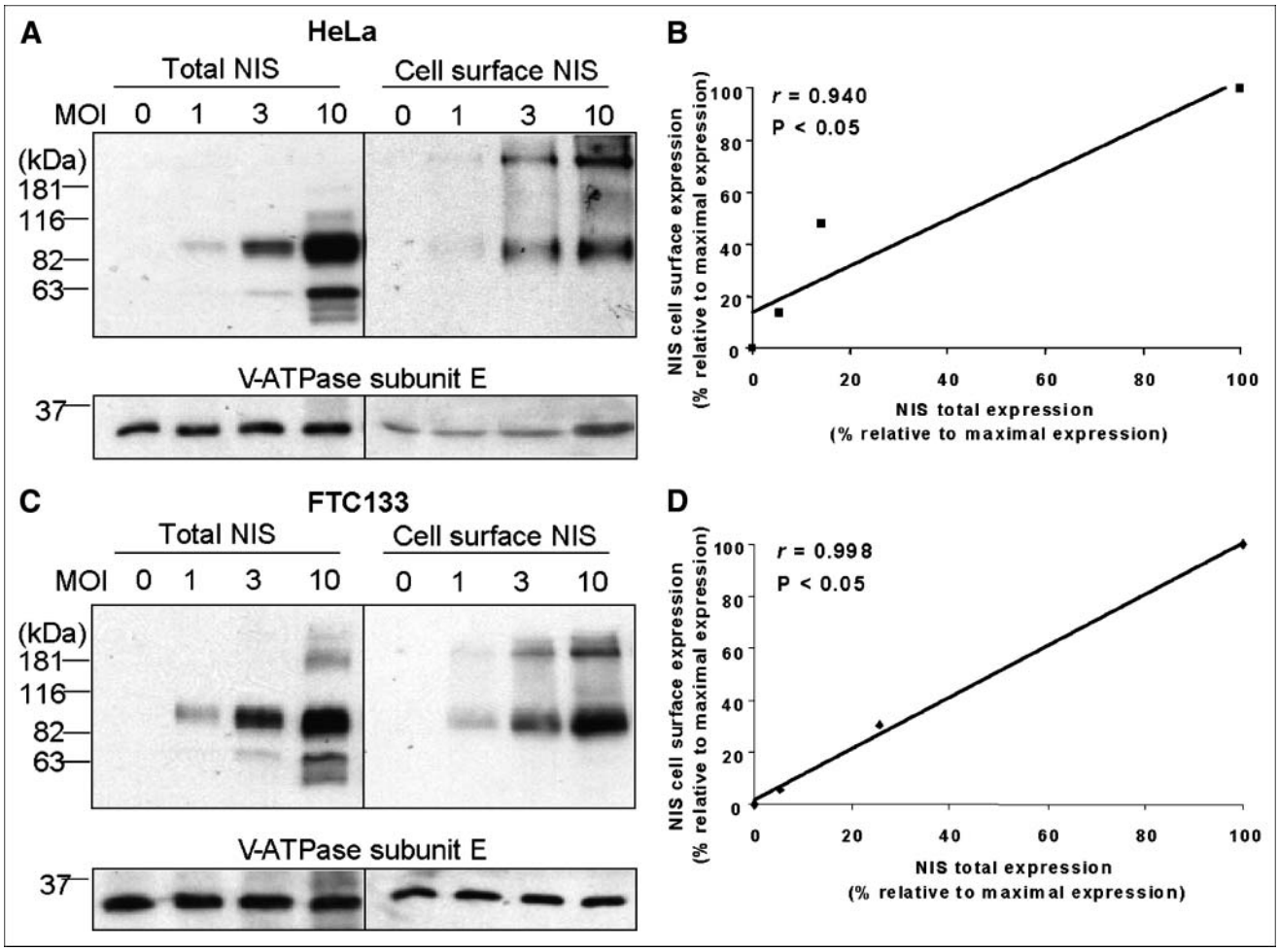

FIGURE 5. Recombinant adenovirus confers high NIS protein levels in both parental FTC133 cells and parental HeLa cells. (A and C) Western blot analysis showed that NIS protein levels are comparable between infected HeLa cells (A) and infected FTC133 cells (C). Both cells were infected with recombinant adenovirus for 48 h, with various multiplicity of infection. Equal loading of proteins was normalized with V-ATPase. Exposure time for detecting NIS protein in both cells was 5 s. Results are representative of 2 independent experiments. (B and D) Regression analysis indicates linear relationship between total NIS protein levels and cell-surface NIS levels in both infected HeLa cells (B) and infected FTC133 cells (D). Densitometric analysis was performed to determine normalized total NIS protein levels and cell-surface NIS levels. Maximally induced total NIS protein levels and maximally induced cell-surface NIS levels were designated as 100%, and other values were assigned relative to maximal levels. Correlation coefficient was determined. $P < 0.05$ indicates statistical significance. MOI = multiplicity of infection.

within a certain range and that a moderate increase in NIS protein level translates into evident increases in radioiodide uptake. Taken together, these findings indicate that a low level of NIS expression may be sufficient to confer radionuclide imaging in vivo, yet NIS is limited to quantifying the expression levels of therapeutic genes within a certain range in vivo.

The finding that a further increase in NIS at the cell surface does not translate into further increases in radioiodide uptake is interesting. Indeed, the degree of NIS-mediated radioiodide uptake in cultured cells is most likely limited by many other factors, such as the availability of substrates, I^- and Na^+. Studies have shown that the initial rate of radioiodide uptake in cultured cells expressing high levels of exogenous NIS could be further increased by increasing the concentrations of Na^+ and I^- in cultured medium (*34,35*). In this study, we showed that steady-state radioiodide uptake could also be further increased by increasing the concentrations of I^- in cultured medium (data not shown). It will be important to further evaluate whether this phenomenon occurs in vivo—a very different microenvironment from that of cell cultures. It is also interesting to note that equivalent NIS cell-surface levels were not associated with equivalent degrees of radioiodide uptake among the different cell types. Different cells may differ in their membrane potential, Na^+/K^+ gradient, influx/efflux kinetics, iodide organification, and so forth. Our data showed that the rate of iodide efflux was not different among FTC133, HeLa, and PC12 cells. It is not surprising that FTC133 cells had a rapid rate of iodide efflux, because thyroid peroxidase, which facilitates iodide organification, is not expressed is this cell (*36*). It will be of physiologic

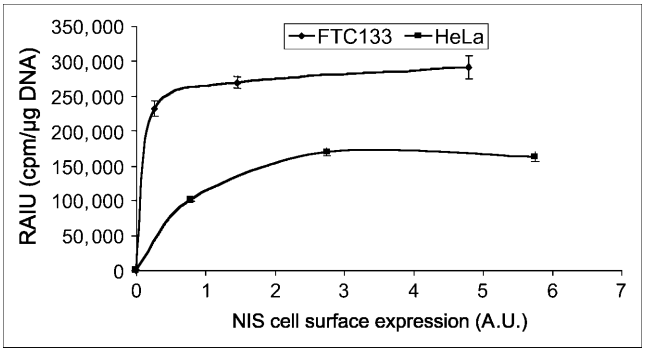

FIGURE 6. Radioiodide uptake was higher in infected FTC133 cells than infected HeLa cells at any equivalent NIS cell-surface levels. Arbitrary values of cell-surface NIS levels were normalized with cell-surface V-ATPase levels and then correlated with corresponding radioiodide uptake. Results are representative of 2 independent experiments. Consistent with finding using TetOn/NIS cells, extent of radioiodide uptake is not further increased by cell-surface NIS levels beyond a certain range. A.U. = arbitrary units; RAIU = radioiodide uptake.

and clinical significance to identify the non-NIS cellular factors that limit the extent of radioiodide uptake.

The rapid efflux of radiotracer in cultured cells indicates that the application of NIS as an imaging reporter gene in cells lacking iodine organification may be compromised. However, $^{99m}TcO_4$, an alternative substrate of NIS that does not become organified or trapped in the thyroid, has been used routinely in the clinic to image the thyroid (7). In addition, exogenous NIS expression in various nonthyroid cells that lack iodide organification has successfully been imaged by radioiodide in vivo (*7–15*). Nevertheless, strategies to enhance radioiodine trapping will be most useful to amplify the imaging signal for NIS as an imaging reporter gene in vivo. In particular, it would be most important to examine ways to increase radioiodide retention if NIS is to be used as a therapeutic gene to facilitate targeted radioiodine therapy.

The human NIS gene has several qualities that make it an ideal imaging reporter gene. First, it is not a foreign gene; hence, NIS is nonimmunogenic. Second, the tissue expression profile of endogenous NIS is limited; as a result, exogenous NIS function can be imaged in a wide variety of nonthyroidal tissues or in thyroid cancer that has lost NIS expression. Third, NIS mediates the uptake of radioisotopes; therefore, complicated synthesis and labeling of substrate molecules is not required for imaging. Fourth, the radioisotopes used are highly selective to NIS-expressing cells; this selectivity reduces interference from unwanted background signal. Fifth, NIS-mediated radiotracer uptake displays rapid background clearing. Consequently, in vivo imaging of NIS-expressing cells can be performed as soon as 30 min after administration of the radioisotope. Finally, the adverse effects of free radioiodine are minimal. It is routinely administered to patients with hyperthyroidism or thyroid cancer for both imaging and therapeutic purposes.

In summary, we showed that the extent of radioiodide uptake generally correlates with NIS protein levels within a certain range; however, the extent of NIS-mediated radioiodide uptake could be modulated by other cellular factors yet to be identified. Our finding that further increases in NIS cell-surface levels do not further increase the extent of radioiodide uptake indicates an inherent capacity of maximal radioiodide uptake in a given cell type. Our study reiterates the following important questions that are highly clinically relevant: What is the optimum NIS protein level for maximal radioiodide uptake in a selected tissue type? Could the maximal radioiodide uptake be further increased in a given tissue type, provided that the non-NIS cellular factors could be identified and modified?

CONCLUSION

Our study suggests that NIS will be useful as an imaging reporter gene to ascertain that the therapeutic gene is localized to the correct tissue and to monitor the expression levels and duration of the therapeutic gene.

ACKNOWLEDGMENTS

We thank Dr. Anjli Venkateswaran for preparation of the HeLa and PC12 doxycycline inducible cell lines. We also thank Dr. Beth Lee for providing us with an antibody against the E subunit of V-ATPase. This work was supported by grant NIBIB 1 R01 EB001876-01 from the National Institutes of Health.

REFERENCES

1. Kaneda Y. Gene therapy: a battle against biological barriers. *Curr Mol Med.* 2001;1:493–499.
2. Phillips AJ. The challenge of gene therapy and DNA delivery. *J Pharm Pharmacol.* 2001;53:1169–1174.
3. Urbain JL. Reporter genes and imagene. *J Nucl Med.* 2001;42:106–109.
4. Allport JR, Weissleder R. In vivo imaging of gene and cell therapies. *Exp Hematol.* 2001;29:1237–1246.
5. Jacobs A, Braunlich I, Graf R, et al. Quantitative kinetics of [^{124}I] FIAU in cat and man. *J Nucl Med.* 2001;42:467–475.
6. Eskandari S, Loo DD, Dai G, et al. Thyroid Na^+/I^- symporter, mechanism, stoichiometry, and specificity. *J Biol Chem.* 1997;272:27230–27238.
7. Shen DH, Kloos RT, Mazzaferri EL, et al. Sodium iodide symporter in health and disease. *Thyroid.* 2001;11:415–425.
8. Cho JY, Shen DH, Yang W, et al. In vivo imaging and radioiodine therapy following sodium iodide symporter gene transfer in animal model of intracerebral gliomas. *Gene Ther.* 2002;9:1139–1145.
9. Shen DH, Marsee DK, Schaap J, et al. Effects of dose, intervention time, and radionuclide on sodium iodide symporter (NIS)-targeted radionuclide therapy. *Gene Ther.* 2004;11:161–169.
10. Marsee DK, Shen DH, MacDonald LR, et al. Imaging of metastatic pulmonary tumors following NIS gene transfer using single photon emission computed tomography. *Cancer Gene Ther.* 2004;11:121–127.
11. Groot-Wassink T, Aboagye EO, Glaser M, et al. Adenovirus biodistribution and noninvasive imaging of gene expression in vivo by positron emission tomography using human sodium/iodide symporter as reporter gene. *Hum Gene Ther.* 2002;13:1723–1735.
12. Shin JH, Chung JK, Kang JH, et al. Feasibility of sodium/iodide symporter gene as a new imaging reporter gene: comparison with HSV1-tk. *Eur J Nucl Med Mol Imaging.* 2004;31:425–432.
13. Groot-Wassink T, Aboagye EO, Wang Y, et al. Quantitative imaging of Na/I symporter transgene expression using positron emission tomography in the living animal. *Mol Ther.* 2004;9:436–442.
14. Niu G, Krager KJ, Graham MM, et al. Noninvasive radiological imaging of pulmonary gene transfer and expression using the human sodium iodide symporter. *Eur J Nucl Med Mol Imaging.* 2005;32:534–540.

15. Lee KH, Kim HK, Paik JY, et al. Accuracy of myocardial sodium/iodide symporter gene expression imaging with radioiodide: evaluation with a dual-gene adenovirus vector. *J Nucl Med.* 2005;46:652–657.
16. Smanik PA, Liu Q, Furminger TL, et al. Cloning of the human sodium iodide symporter. *Biochem Biophys Res Commun.* 1996;226:339–345.
17. La Perle KM, Shen D, Buckwalter TL, et al. In vivo expression and function of the sodium iodide symporter following gene transfer in the MATLyLu rat model of metastatic prostate cancer. *Prostate.* 2002;50:170–178.
18. Cho JY, Xing S, Buckwalter TL, et al. Expression and activity of human Na^+/I^- symporter in human glioma cells by adenovirus-mediated gene delivery. *Gene Ther.* 2000;7:740–749.
19. Boland A, Ricard M, Opolon P, et al. Adenovirus-mediated transfer of the thyroid sodium/iodide symporter gene into tumors for a targeted radiotherapy. *Cancer Res.* 2000;60:3484–3492.
20. Mandell RB, Mandell LZ, Link CJ Jr. Radioisotope concentrator gene therapy using the sodium/iodide symporter gene. *Cancer Res.* 1999;59:661–668.
21. Lee WW, Lee B, Kim SJ, et al. Kinetics of iodide uptake and efflux in various human thyroid cancer cells by expressing sodium iodide symporter gene via a recombinant adenovirus. *Oncol Rep.* 2003;10:845–849.
22. Petrich T, Knapp WH, Potter E. Functional activity of human sodium/iodide symporter in tumor cell lines. *Nuklearmedizin.* 2003;42:15–18.
23. Marsee DK, Venkateswaran A, Tao H, et al. Inhibition of heat shock protein 90, a novel RET/PTC1-associated protein, increases radioiodide accumulation in thyroid cells. *J Biol Chem.* 2004;279:43990–43997.
24. Levy O, Dai G, Riedel C, et al. Characterization of the thyroid Na^+/I^- symporter with an anti-COOH terminus antibody. *Proc Natl Acad Sci USA.* 1997;94:5568–5573.
25. Dohan O, De la Vieja A, Paroder V, et al. The sodium/iodide symporter (NIS): characterization, regulation, and medical significance. *Endocr Rev.* 2003;24:48–77.
26. Mitrofanova E, Unfer R, Vahanian N, et al. Rat sodium iodide symporter for radioiodide therapy of cancer. *Clin Cancer Res.* 2004;10:6969–6976.
27. Castro MR, Bergert ER, Goellner JR, et al. Immunohistochemical analysis of sodium iodide symporter expression in metastatic differentiated thyroid cancer: correlation with radioiodine uptake. *J Clin Endocrinol Metab.* 2001;86:5627–5632.
28. Tonacchera M, Viacava P, Agretti P, et al. Benign nonfunctioning thyroid adenomas are characterized by a defective targeting to cell membrane or a reduced expression of the sodium iodide symporter protein. *J Clin Endocrinol Metab.* 2002;87:352–357.
29. Pohlenz J, Duprez L, Weiss RE, et al. Failure of membrane targeting causes the functional defect of two mutant sodium iodide symporters. *J Clin Endocrinol Metab.* 2000;85:2366–2369.
30. Pohlenz J, Rosenthal IM, Weiss RE, et al. Congenital hypothyroidism due to mutations in the sodium/iodide symporter: identification of a nonsense mutation producing a downstream cryptic 3′ splice site. *J Clin Invest.* 1998;101:1028–1035.
31. Kosugi S, Okamoto H, Tamada A, et al. A novel peculiar mutation in the sodium/iodide symporter gene in Spanish siblings with iodide transport defect. *J Clin Endocrinol Metab.* 2002;87:3830–3836.
32. Pohlenz J, Medeiros-Neto G, Gross JL, et al. Hypothyroidism in a Brazilian kindred due to iodide trapping defect caused by a homozygous mutation in the sodium/iodide symporter gene. *Biochem Biophys Res Commun.* 1997;240:488–491.
33. Zhang Z, Liu YY, Jhiang SM. Cell surface targeting accounts for the difference in iodide uptake activity between human Na+/I− symporter and rat Na+/I− symporter. *J Clin Endocrinol Metab.* 2005;Aug 16 [Epub ahead of print].
34. Levy O, De la Vieja A, Ginter CS, et al. N-linked glycosylation of the thyroid Na^+/I^- symporter (NIS): implications for its secondary structure model. *J Biol Chem.* 1998;273:22657–22663.
35. Zuckier LS, Dohan O, Li Y, et al. Kinetics of perrhenate uptake and comparative biodistribution of perrhenate, pertechnetate, and iodide by NaI symporter-expressing tissues in vivo. *J Nucl Med.* 2004;45:500–507.
36. Smit JW, Schroder-van der Elst JP, Karperien M, et al. Iodide kinetics and experimental ^{131}I therapy in a xenotransplanted human sodium-iodide symporter-transfected human follicular thyroid carcinoma cell line. *J Clin Endocrinol Metab.* 2002;87:1247–1253.

JNM The Journal of NUCLEAR MEDICINE

Correlation of Na^+/I^- Symporter Expression and Activity: Implications of Na^+/I^- Symporter as an Imaging Reporter Gene

Douangsone D. Vadysirisack, Daniel H. Shen and Sissy M. Jhiang

J Nucl Med. 2006;47:182-190.

The Journal of Nuclear Medicine is published monthly.
SNMMI | Society of Nuclear Medicine and Molecular Imaging
1850 Samuel Morse Drive, Reston, VA 20190.
(Print ISSN: 0161-5505, Online ISSN: 2159-662X)

SNMMI SOCIETY OF NUCLEAR MEDICINE AND MOLECULAR IMAGING